Polymer Chemistry

One-Pot Synthesis of Linear Triblock Terpolymers and their Aqueous Self-Assembly

Journal:	*Polymer Chemistry*
Manuscript ID	PY-ART-01-2021-000054.R1
Article Type:	Paper
Date Submitted by the Author:	25-Feb-2021
Complete List of Authors:	Ahmed, Eman; New York University, Molecular Design Institute and Womble, C.; New York University, Molecular Design Institute and Cho, Jinwon; Georgia Institute of Technology, e. School of Materials Science and Engineering Dancel Manning, Kristen; New York University Langone , Rice, William; NYU Langone Health Jang, Seung Soon; Georgia Institute of Technology, Materials Science and Engineering Weck, Marcus; New York University, Molecular Design Institute and

ARTICLE

a

One-Pot Synthesis of Linear Triblock Terpolymers and their Aqueous Self-Assembly

Eman Ahmed,[a] C. Tyler Womble,[a] Jinwon Cho,[b] Kristen Dancel-Manning,[c] Dr. William J. Rice,[d] Seung Soon Jang*[b] and Marcus Weck*[a]

Compartmentalized micelles are prepared through the self-assembly of linear triblock terpolymers containing hydrophilic (**H**), lipophilic (**L**), and fluorophilic (**F**) domains. The triblock copolymers were synthesized via living ring-opening metathesis polymerization (ROMP) of norbornene-based monomers. Our terpolymer design offers a facile approach for the synthesis of the target materials with fast polymerization kinetics, complete block incorporation and control over block sequence. Various triblock terpolymers are prepared with variations in block sequence and block ratio and self-assembled in aqueous media. Interaction parameter (χ) values between each block are determined using a Flory-Huggins based computational model. "Core-shell-corona", "disk-like", "raspberry-like" and "worm-like" morphologies are observed through cryogenic transmission electron microscopy and dissipative particle dynamics simulations.

INTRODUCTION

A long-standing goal of polymer science is to simulate and harness the efficiency of chemical processes found in nature.[1,2] A key example is molecular self-assembly, a process ubiquitous in biological systems.[3] The internal organization of eukaryotic cells has inspired the assembly of nanostructures with spatially segregated compartments as a strategy towards the fabrication of next-generation functional materials for applications in catalysis and targeted substrate uptake.[4–11] Mimicry of the structural complexity found in natural systems where multiple domains or compartments coexist within a single structure, however, is synthetically challenging.[12] One strategy for preparing materials with multiple distinct domains is to self-assemble macromolecules into nanostructures.[13] Block copolymers readily undergo microphase separation and their assembly properties in solution have been well studied.[14,15] Changes to monomer structure, polymer block length, and architecture allows for tunability of the desired nanostructure morphology and size.[16–18]

Hydrophilic-hydrophobic diblock copolymers assemble into micelles with two domains: core and corona.[19] Increasing the number of spatially separated domains allows for the formation of complex, nanostructured materials, such as multicompartment micelles (MCMs).[16,20] Incorporation of a third block that is mutually incompatible with the others leads to the formation of additional domains upon assembly in solution.[21–26] Commonly, a fluorine-rich block provides the required microphase separation from the water soluble (hydrophilic) and oil soluble (lipophilic) polymer blocks. MCMs bearing fluorophilic (**F**), lipophilic (**L**), and hydrophilic (**H**) segments have previously been reported and their aggregation behaviour in solution led to a wealth of three-dimensional nanostructures.[22, 23, 25–31]

Most MCMs have been prepared from ionic or Reversible Deactivation Radical Polymerization (RDRP) methods and reports of MCMs assembled from polymers containing functional handles remain limited.[16] Ionic polymerizations limit the scope of available functionalities that can be incorporated into the polymer chain without significant post-polymerization modifications.[27,28] RDRP yields well-defined macromolecules and has adequate functional group tolerance; the presence of termination events, however, necessitates stopping the polymerization at low conversions and purification steps are required after each block addition.[29] Additionally, RDRP has slow polymerization kinetics and require high reaction temperatures.[28]

Living Ring-Opening Metathesis Polymerization (ROMP) is a powerful method for the preparation of well-defined polymers with exceptional control over the composition and architecture of the scaffold.[30–32] ROMP has a high functional group tolerance and rapid polymerization times, on a time scale of minutes in both water and organic solvents.[31,33–35] Its living nature ensures full monomer consumption and enables the polymerization of multi-block copolymers in one-pot by sequential monomer addition.[36,37] ROMP also allows for simple adjustment of block lengths and block sequence resulting in easy tuning of polymer properties. Furthermore, ROMP yields an unsaturated polymer

[a] *Molecular Design Institute, Department of Chemistry, New York University, New York, NY, 10003, United States. E-mail:* marcus.weck@nyu.edu
[b] *School of Materials Science and Engineering, Georgia Institute of Technology, 771 Ferst Dr., Atlanta, GA 30332-0245, United States. E-mail:* seungsoon.jang@mse.gatech.edu
[c] *OCS Microscopy Core, New York University Langone Medical Center, New York, New York 10016, United States.*
[d] *Cryo-Electron Microscopy Laboratory, New York University Langone Medical Center, New York, New York 10016, United States.*
Electronic Supplementary Information (ESI) available: Experimental protocols and characterization data.

backbone that offers additional sites for targeted functionalization.[38] In recent years, ROMP has gained unprecedented popularity for the synthesis of functional amphiphilic block copolymers for biomedical applications.[39] ROMP has not yet been used for the synthesis of linear terpolymers with lipophilic, fluorophilic and hydrophilic blocks and their subsequent self-assembly into MCMs remains to be investigated.

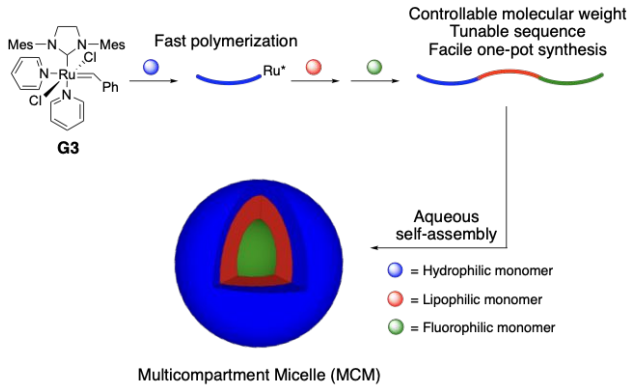

Figure 1. Schematic representation of the one-pot synthesis of triblock terpolymers by ROMP and aqueous self-assembly into multicompartment micelles.

We have recently described the formation of MCMs using bottle brush copolymers with four incompatible domains prepared by ROMP.[17] The complex nature of the bottlebrush copolymers limited the distinction between the four blocks via cryogenic transmission electron microscopy (cryo-TEM). Herein, we advance the scope of multicompartment micelles by preparing triply amphiphilic linear block copolymers from ROMP of norbornenes in one-pot (**Figure 1**). The triblock copolymers are based on a water-soluble monomer (**H**), a norbornene with a six-carbon chain (**L**) and a norbornene with a fluorine rich side-chain (**F**) that phase separate in aqueous solution to yield MCMs with three distinct domains. Interaction parameter (χ) values determined using a Flory-Huggins based computational model confirmed phase separation between the amphiphilic polymers. Cryo-TEM and dissipative particle dynamic (DPD) simulations were used to observe the self-assembly behaviour of micelles. Our facile approach enables the aqueous assembly of MCMs with tunable morphologies for potential applications in cascade catalysis and biomedicine.

RESULTS AND DISCUSSION

Monomer syntheses. Norbornene-based monomers with fluorophilic, lipophilic, and hydrophilic moieties were synthesized according to modified literature procedures (see Supporting Information for experimental details).[40–43] Monomer selection is critical for designing triblock copolymers that phase separate in solution.[5] It has been computationally predicted that monomer properties can have a significant effect on macromolecular assembly and result in altered morphologies.[44] We selected monomers based on appropriate homopolymer solubility and with non-ionic, short side-chains. The lipophilic monomer (**L**) was synthesized by treating exo-norbornene dicarboxylic anhydride with hexylamine.[42] The fluorophilic monomer (**F**) was synthesized from the retro Diels-Alder/Diels-Alder reaction of dicyclopentadiene and 1*H*,1*H*,2*H*-perfluoro-1-hexene.[40,41] Following distillation of the product, the monomer was obtained as a 3:1 *endo*/*exo* mixture of isomers. There are few reports of water-soluble poly(norbornene)s that do not have poly(ethylene glycol), cationic, or zwitterionic side-chains.[45,46] Tew and co-workers have reported the living ROMP of a tertiary amine functionalized norbornene.[43] Following the Tew strategy, *exo*-oxanorbornene dicarboxylic anhydride was transformed into the hydrophilic monomer (**H**).

Polymer syntheses. Triblock terpolymers were synthesized using Grubbs' initiator (**G3**) in a one-pot polymerization by sequential monomer addition (**Scheme 1**, see Supporting Information for full experimental details).[47] The polymerization times of each monomer were determined from kinetics experiments using ^{1}H NMR spectroscopy. The apparent propagation rate constant (k_p^{app}) was calculated from a pseudo-first order plot of conversion vs. time (Figure S1). Full conversion of **F** in toluene-d8 and **L** in CD_2Cl_2 was observed after four minutes with k_p^{app} of 0.016 s^{-1} and 0.03 s^{-1}, respectively (Figures S3-4). **H** required over 10 minutes in CD_2Cl_2 for full monomer consumption (k_p^{app} = 0.005 s^{-1}) (Figure S2). Thus, 15 minutes were allocated for complete monomer consumption of **F** and **L** and 40 minutes for **H**. α,α,α-Trifluorotoluene was used as a co-solvent to maintain control over the polymerization, because of the limited solubility of the fluorinated block. ^{1}H NMR spectroscopy confirmed full monomer consumption based on the absence of norbornene vinyl signals at 6.44 ppm (**H**), 6.27 ppm (**L**), or 6.10 and 5.88 ppm (**F**) after subsequent monomer addition (**Figure 2**).

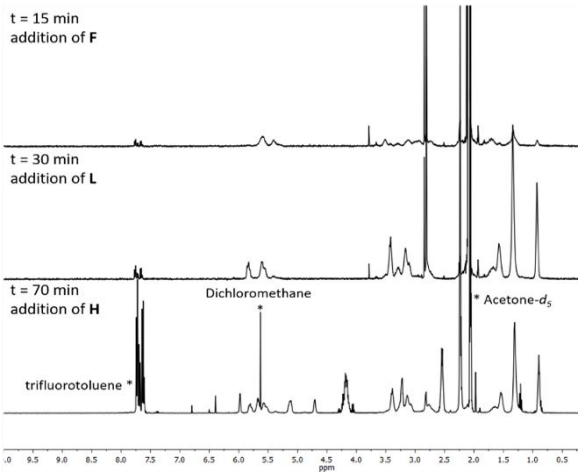

Figure 2. Stacked ^{1}H NMR spectra of aliquots taken from the crude polymerization mixture after each monomer addition (**Series 1b**, **Table 1**). The spectra were obtained in Acetone-d_6, 500 MHz.

Scheme 1. Schematic representation of the synthesis of triblock terpolymers by ROMP

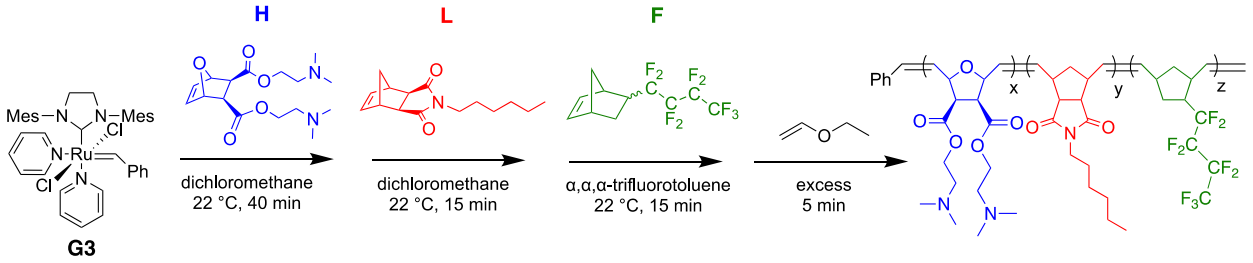

Adjusting the polymer block sequence can result in dramatic changes to the morphology of self-assembled nanostructures.[48,49] Our synthetic strategy enabled alteration of the block arrangement by simply changing the order of monomer addition to yield polymers with three sequences: **F – H – L**, **F – L – H**, **L– F – H**. A library of nine polymers (**Table 1**) with varying block orders and block ratios were synthesized to determine the impact on micelle morphology. The subscripted values in the triblock sequence denote the degree of polymerization of each block. In **Series 1** and **2**, the ratio of the hydrophilic to hydrophobic segments is 1:1. A balance between the volume fraction of the hydrophilic to hydrophobic segments is pivotal in determining the size of the self-assembled micelles.[50] In **Series 3**, the ratio of hydrophilic to hydrophobic segments is decreased (0.6:1) to determine the impact of interfacial curvature on the self-assembled structures.[23]

Polymer			Polymerization Composition								
			% F		% L		% H		M_n (kDa)		
			Theoretical	Experimental[a]	Theoretical	Experimental[b]	Theoretical	Experimental[c]	GPC[d]	Theoretical[e]	$Đ^d$
Series 1	a	$F_{75}-H_{200}-L_{125}$	18.8	15.5	31.2	40.0	50	47.3	48.2	119.6	1.11
	b	$F_{75}-L_{125}-H_{200}$	18.8	18.3	31.2	42.7	50	40.8	65.7	119.6	1.06
	c	$L_{125}-F_{75}-H_{200}$	18.8	16.9	31.2	42.0	50	42.5	70.5	119.6	1.11
Series 2	a	$F_{100}-H_{400}-L_{300}$	12.5	11.0	37.5	48.7	50	42.5	125.6	236.0	1.17
	b	$F_{100}-L_{300}-H_{400}$	12.5	12.7	37.5	48.7	50	42.5	128.9	236.0	1.11
	c	$L_{300}-F_{100}-H_{400}$	12.5	7.0	37.5	46.3	50	47.3	101.6	236.0	1.07
Series 3	a	$F_{125}-H_{300}-L_{375}$	15.6	9.9	46.9	57.3	37.5	34.0	159.7	230.0	1.23
	b	$F_{125}-L_{375}-H_{300}$	15.6	19.7	46.9	52.3	37.5	32.3	122.3	230.0	1.10
	c	$L_{375}-F_{125}-H_{300}$	15.6	18.3	46.9	52.7	37.5	30.5	131.8	230.0	1.10

Table 1. Triblock terpolymer composition

[a]Determined via ^{1}H NMR spectroscopy (Acetone-d_6, 500 MHz) from the integration of signals of the *cis* vinyl protons δ (5.43–5.23 ppm) in comparison to the backbone vinyl protons signals (δ 6.04–5.23 ppm) (see Supporting Information, e.g., calculations). [b]Determined from the integration of signals of the methyl protons δ (0.99–0.78 ppm) compared to the signals of the backbone vinyl protons. [c]Determined from the integration of the signals of the –OCH_2– protons δ (4.26–4.07 ppm) compared to the signals of the backbone vinyl signals. [d]THF was used as the eluent for GPC analysis and the differential refractometer trace (dRI) was used to determine the M_n and $Đ$ values. [e]Theoretical polymer composition and molecular weights were calculated from the monomer feed ratios.

^{1}H and ^{19}F{^{1}H} NMR spectroscopies were used to ensure the composition of the final polymers closely matched the monomer feed ratio (**Table 1**). Broadened signals in the ^{19}F{^{1}H} spectra confirmed the presence of the **F** block in the final polymer. Integration of signals unique to each monomer in the ^{1}H NMR spectrum relative to the integration of the total vinyl signals (6.08 – 5.26 ppm) was used to calculate the relative amounts of **F**, **L**, and **H** (see Supporting Information). The feed ratio of all monomers closely matched the targeted polymer composition.

Gel-permeation chromatography (GPC) was used to characterize the polymers. GPC chromatograms of the homopolymers displayed monomodal traces with low dispersities (Figure S15). The experimental molecular weights of the triblock terpolymers were approximately half the expected value (**Table 1**). We attribute this discrepancy to the unfavourable interactions between the hydrophilic block and the hydrophobic column that impacts the hydrodynamic volume of the triblock copolymer (Figure S24).[51] The molecular weight evolution with each monomer

addition was also investigated using GPC for polymers **2a-c**. Though the polymer traces were monomodal with narrow molecular weight distributions, after each addition, an increase in the molecular weight was only observed for **2b** (Figure S16). Polymers **2a** and **2c** resulted in a decrease in molecular weight with subsequent block addition confirming our hypothesis of column interactions.

Thermal analyses were conducted to determine glass-transition temperatures of the homopolymers and **2a**. Thermal gravimetric analysis (TGA) confirmed the thermal stability of **2a** up to 220 °C. Differential scanning calorimetry (DSC) of the homopolymers displayed a glass transition temperature (T_g) at ~ 72 °C for **F** and ~ 91 °C for **L** (Figure S18). First or second order transitions were not obvious for homopolymer **H**. Polymer **2a** showed a T_g at ~ 61 °C and 94 °C confirming the presence of **F** and **L** respectively (Figure S18).

χ Parameter Calculations. Using the Flory-Huggins solution theory, domain segregation between the polymers was confirmed by computing the χ-parameters for the monomers.[52] The computational method used here to determine the χ values was developed in a previous study.[53] The χ-parameter is defined by the Gibbs free energy of mixing and expressed as follows;

$$\chi_{ij} = \frac{\Delta w_{ij}}{RT}$$

where $\chi_{i,j}$ is the χ-parameter between polymer i and j, and Δw_{ij} is a mixing energy of polymer i and j which is defined as;

$$\Delta w_{ij} = \frac{1}{2} V_{ref}\left[(Z_{ij} + Z_{ji})\frac{E_{ij}}{V_{ij}} - (Z_{ii}\frac{E_{ii}}{V_{ii}} + Z_{jj}\frac{E_{jj}}{V_{jj}})\right]$$

where Z_{ij}, V_{ij}, V_{ref}, and E_{ij} refer to the coordination number of the species j around the species i, the volume enclosed by the Connolly surface over the combined pair of molecules i and j, reference volume, and interaction energy between individual molecules of species i and j, respectively.

Table 2. Computational evaluation of χ-parameter values for each monomer pair, and monomer-water.

χ_{ij}	H	L	F	Water
H		0.481	0.519	0.482
L			0.301	0.892
F				0.931
Water				

Our results (**Table 2**) indicate that the **F**-Water mixture exhibits the highest χ-parameter ($\chi_{F,Water} = 0.931$), followed by **L**-Water ($\chi_{L,Water} = 0.892$) and **H**-Water ($\chi_{H,Water} = 0.482$). As expected, the χ values confirm that the fluorophilic monomer is the most hydrophobic. Phase separation between **H** and **F** blocks is expected according to $\chi_{H,F}$. A high χ-parameter ($\chi_{H,L} = 0.519$) implies that block **H** is immiscible with block **F**, thus self-assembling into a core-shell micelle. In fact, core-shell morphology is experimentally confirmed in the diblock **H_{200} – F_{50}** copolymers (**Figure 3, 2**). Likewise, $\chi_{H,L}$ = 0.481 indicates phase separation between **H** and **L** monomers and agrees with the experimental cryo-TEM images of the diblock copolymer **H_{200} – L_{150}** (**Figure 3, 1)**.

Micelle Formation and Characterization via cryo-TEM. After the synthesis of the triblock terpolymers, we investigated their aqueous self-assembly. Micellar nanostructures were formed by the dissolution of the polymers (10 mg) in acetone (1 mL) and dialysis against water for one week to obtain a final concentration of 10 mg/mL (see Supporting Information). The hydrodynamic diameters (D_h) of the nanostructures were determined via Dynamic Light Scattering (DLS) analysis (Figure S18). The size of the nanostructures ranged from 60–250 nm and uniform particles were obtained, polydispersity index (PDI)<0.7 (**Table 3**).[54] Upon changing the block order, **Series 1** showed minimal variance in the micelle sizes. Larger particles were observed in **Series 2** and **3**, owing to the higher degree of polymerization. Larger nanoparticle sizes in **Series 3** can also be attributed to the long insoluble blocks that result in micellar clusters formed by secondary aggregation of primary micelles.[55]

Table 3. Particle size distribution of self-assembled triblock terpolymers determined by DLS.

Polymer		Composition	$D_{h,avg}$ (nm)	PDI
Series 1	a	$F_{75}-H_{200}-L_{125}$	77 ± 1	0.29
	b	$F_{75}-L_{125}-H_{200}$	62 ± 1	0.21
	c	$L_{125}-F_{75}-H_{200}$	65 ± 1	0.28
Series 2	a	$F_{100}-H_{400}-L_{300}$	194 ± 1	0.15
	b	$F_{100}-L_{300}-H_{400}$	98 ± 1	0.45
	c	$L_{300}-F_{100}-H_{400}$	145 ± 1	0.56
Series 3	a	$F_{125}-H_{300}-L_{375}$	134 ± 1	0.21
	b	$F_{125}-L_{375}-H_{300}$	246 ± 4	0.01
	c	$L_{375}-F_{125}-H_{300}$	169 ± 1	0.32

Cryo-TEM was used to image the morphology of the self-assembled nanostructures. The particle sizes determined by DLS were larger than the ones observed by cryo-TEM because the former accounts for the hydrodynamic diameter, while in the latter it is difficult to visualize the solvated hydrophilic corona due to limited contrast with the ice matrix.[56]

In order to confirm the phase separation of the **L** and **F** blocks in aqueous media we assembled diblock copolymers into micelles. Microphase separation was

apparent in the cryo-TEM images of diblock copolymers, $\mathbf{H_{200} - L_{150}}$ and $\mathbf{H_{200} - F_{50}}$ displaying "core-shell" morphologies (**Figure 3**).

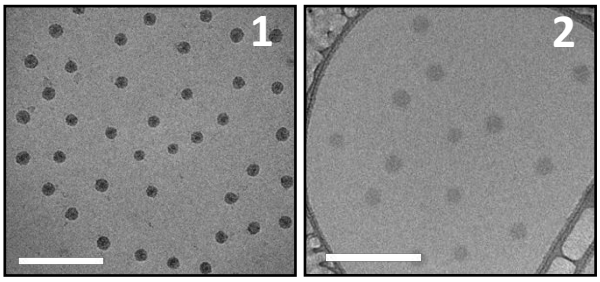

Figure 3. Cryo-TEM images of diblock copolymers assembled in aqueous media. **1**. $\mathbf{H_{200} - L_{150}}$; **2**. $\mathbf{H_{200} - F_{50}}$. Scale bars: 100 nm

Cryo-TEM images of the triblock terpolymers revealed characteristic features depending on their block ratio, block sequence, degree of polymerization, and hydrophobic-hydrophilic balance. Due to the high contrast of the fluorinated domain, a low block ratio is needed for the fluorinated block with respect to the lipophilic segment, in order to observe phase separation. Polymers with a fluorophilic to lipophilic block ratio of 1:1 and 1.5:1 resulted in spherical micelles with no clear phase contrast (Figure S20-S21). Despite a low fluorophilic to hydrophilic ratio, the polymers in **Series 1** displayed spherical micelles with no distinct microphase separation in the core (**Figure 4, Series 1a-c**).

Upon increasing the degree of polymerization in **Series 2**, a "disk-like"[5,57] morphology was observed for polymer **2a** with an **F – H – L** sequence. The large dark core can be assigned to the fluorinated domain surrounded by the lipophilic shell.[25,56] Fluorine containing polymers can access the "super strong segregation limit" (SSSL) whereby the large interfacial energy exceeds the entropic penalty to stretch the core blocks.[5] This results in a stretched core with a flat interface forming "disk-like" micelles.[16,57] Polymers **2b** and **2c** yielded "core-shell-corona"[5] spherical particles and it was difficult to distinguish between the two hydrophobic domains. We attribute this observation to the burial of the fluorophilic domain within the inner part of the micelle, because contact between the fluorinated block and water are much less favourable than water and the lipophilic block. Since cryo-TEM provides a two-dimensional projection of a three-dimensional object, we are unable to differentiate between the two hydrophobic domains.[25]

In **Series 3,** a disproportion between the volume fraction of the hydrophobic-hydrophilic blocks results in a morphological evolution of spherical particles into aggregates. Polymers **3a** and **3b** assembled into "worm-like"[16] aggregates while polymer **3c** yielded "raspberry-like"[22] nanostructures. In these nanostructures, the darker fluorinated domains were visible. To elucidate the location of the fluorinated block in the "worm-like" aggregates we conducted cryo-electron tomography (cryo-ET). Similar to a "core-shell-corona" micelle, the fluorinated block is buried inside the nanostructure unlike "raspberry-like" micelles where the fluorine rich domain is on the surface (Video S1). Polymers in **Series 3** clearly underline the importance of block order in the location of each domain and micelle assembly.

Micelle Characterization via DPD Simulations. We carried out DPD simulations to investigate the structural variation of triblock terpolymer micelles as a function of block ratio. The repulsion parameters ($\boldsymbol{a_{ij}}$) employed in DPD simulations were obtained via the following equation reported previously.[44,58]

$$a_{ij} = 25 + 3.5\chi_{ij}$$

Through coarse-grained modelling, the same block ratios were employed as described in **Table 2**. The simulation systems were set to have 5% polymer and 95% water, and the simulation box size was defined as 40 × 40 × 40 with a grid spacing of 1.0 and a bead density of 3.0, in which it is known that the DPD repulsion parameter a_{ij} for species i and j has a linear relationship with the corresponding Flory–Huggins χ_{ij}-parameter, as derived by Groot and Warren.[59]

In DPD simulations for polymer **2a**, the fluorophilic domain is in the core of the micelle surrounded by the lipophilic and hydrophilic block (**Figure 5**, **2a**). This is analogous to the "disk-like" micelles that are observed in cryo-TEM (**Figure 4, 2a**) where the micellar core is stretched. In **Figure 5, 2c**, the hydrophilic shell is more dispersed than **2a** comparable to the "core-shell-corona" micelles visible in cryo-TEM (**Figure 4, 2a**). A "worm-like" elongated micelle structure is found for polymer **3a**, where the fluorinated blocks is in the core of the micelle, covered by the lipophilic and hydrophilic domain (**Figure 5**, **3a**). The fluorophilic block is observed on the surface in **Figure 5**, **3c**, corresponding to "raspberry-like" micelles (**Figure 4, 3c**). Ultimately, the simulated triblock terpolymers yield micelle morphology in parallel to the ones observed in cryo-TEM.

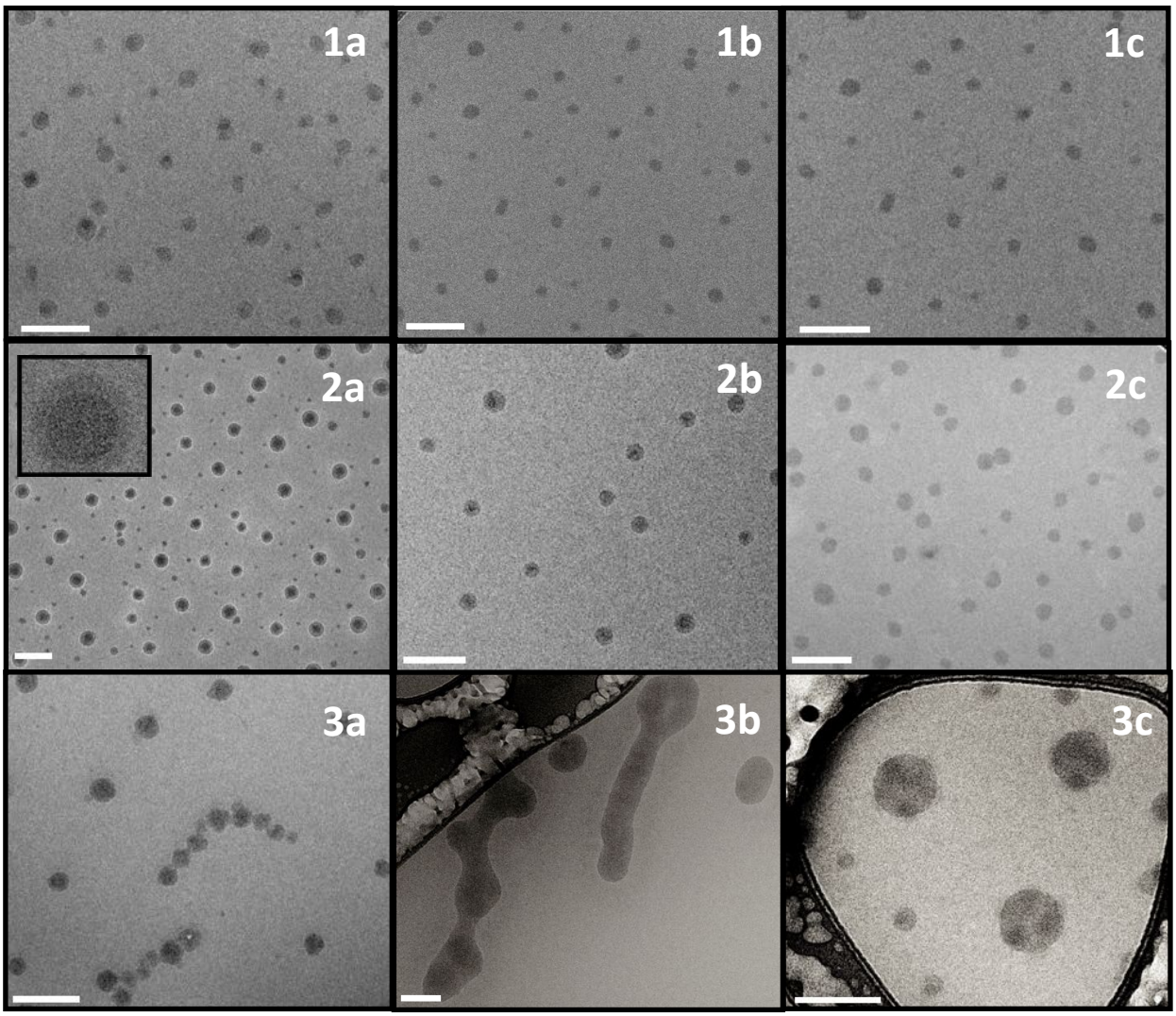

Figure 4. Cryo-TEM images of self-assembled triblock terpolymers corresponding to Table 1 (**Series 1-3**). Scale bars: 100nm

ARTICLE

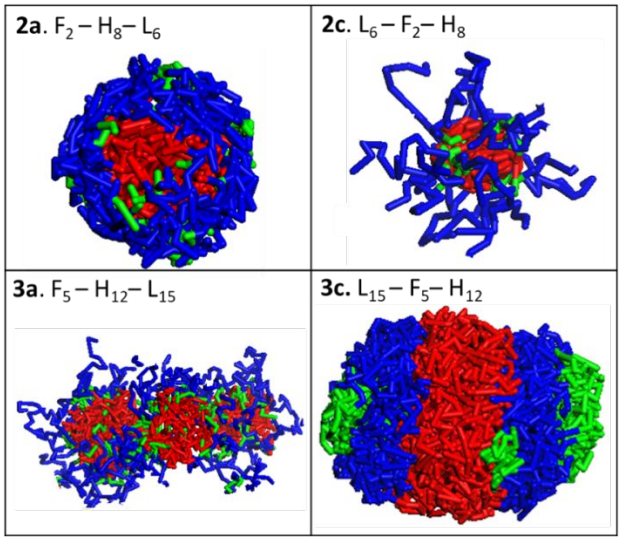

Figure 5. DPD simulation results for the self-assembly of triblock terpolymers. **2a**. $\mathbf{F_2 – H_8 – L_6}$; **2c.** $\mathbf{L_9 – F_3 – H_{12}}$; **3a.** $\mathbf{F_5 – H_{12} – L_{15}}$; **3c.** $\mathbf{L_6 –F_2 – H_8}$. **H**, **L**, and **F** blocks are represented in blue, red and green, respectively.

Conclusion

Triblock terpolymers with hydrophilic, lipophilic, and fluorophilic blocks were synthesized by ROMP. Fast polymerization kinetics enabled simple manipulation of the polymer block ratio and sequence. Phase separation between the monomers was confirmed by computing the χ-parameter. The polymers were assembled into MCMs in water and their morphologies were observed by cryo-TEM and DPD simulations. Block ratio, block sequence, degree of polymerization, and hydrophobic-hydrophilic balance had a substantial influence on the morphology of the nanostructures that ranged from "core-shell-corona" micelles to "disk-like" and "raspberry-like" to "worm-like" structures. The functional group tolerant nature of ROMP can facilitate the incorporation of chemical handles along the backbone, terminal ends and side chain ends of the polymer which can be decorated with catalysts paving the way for the use of MCMs as catalytic nanoreactors.

Conflicts of interest

There are no conflicts to declare

Acknowledgements

Funding provided by the U.S. Department of Energy, Office of Basic Energy Sciences, through Catalysis Science Contract DE-FG02-03ER15459, is gratefully acknowledged. We thank Dr. Michael Peter Kuepfert for thoughtful discussions.

References

1 G. M. Whitesides and B. Grzybowski, Self-Assembly at All Scales, *Science*, 2002, **295**, 2418–2421.
2 G. M. Whitesides and M. Boncheva, Beyond molecules: Self-assembly of mesoscopic and macroscopic components, *Proc. Natl. Acad. Sci. USA* 2002, **99**, 4769–4774.
3 H. Ringsdorf, P. Lehmann and R. Weberskrich, Book of Abstracts, 217th ACS National Meeting; American Chemical Society: Washington, DC.
4 I. W. Hamley, Nanotechnology with Soft Materials, *Angew. Chem. Int. Ed.*, 2003, **42**, 1692–1712.
5 A. H. Gröschel and A. H. E. Müller, Self-assembly concepts for multicompartment nanostructures, *Nanoscale*, 2015, **7**, 11841–11876.
6 P. Tanner, P. Baumann, R. Enea, O. Onaca, C. Palivan and W. Meier, Polymeric vesicles: from drug carriers to nanoreactors and artificial organelles, *Acc. Chem. Res.*, 2011, **44**, 1039–1049.
7 A. Najer, D. Wu, D. Vasquez, C. G. Palivan and W. Meier, Polymer nanocompartments in broad-spectrum medical applications, *Nanomedicine*, 2013, **8**, 425–447.
8 A. Lu and R. K. O'Reilly, Advances in nanoreactor technology using polymeric nanostructures, *Curr. Opin. Biotechnol.*, 2013, **24**, 639–645.
9 T. P. Lodge, A. Rasdal, Z. Li and M. A. Hillmyer, Simultaneous, Segregated Storage of Two Agents in a Multicompartment Micelle, *J. Am. Chem. Soc.*, 2005, **127**, 17608–17609.
10 U. Nayanathara, S. S. Kermaniyan and G. K. Such, Multicompartment Polymeric Nanocarriers for Biomedical Applications, *Macromol. Rapid Commun.*, 2020, **41**, 2000298.
11 T.-L. Nghiem, D. Coban, S. Tjaberings and A. H. Gröschel, Recent Advances in the Synthesis and Application of Polymer Compartments for Catalysis, *Polymers*, 2020, **12**, 2190.

12 J.-F. Lutz, J.-M. Lehn, E. W. Meijer and K. Matyjaszewski, From precision polymers to complex materials and systems, *Nat. Rev. Mater.*, 2016, **1**, 1–14.

13 T. Trantidou, M. Friddin, Y. Elani, N. J. Brooks, R. V. Law, J. M. Seddon and O. Ces, Engineering Compartmentalized Biomimetic Micro- and Nanocontainers, *ACS Nano*, 2017, **11**, 6549–6565.

14 I. I. I. Thomas H. Epps and R. K. O'Reilly, Block copolymers: controlling nanostructure to generate functional materials – synthesis, characterization, and engineering, *Chem. Sci.*, 2016, **7**, 1674–1689.

15 Y. Mai and A. Eisenberg, Self-assembly of block copolymers, *Chem. Soc. Rev.*, 2012, **41**, 5969–5985.

16 A. O. Moughton, M. A. Hillmyer and T. P. Lodge, Multicompartment Block Polymer Micelles, *Macromolecules*, 2012, **45**, 2–19.

17 E. Ahmed, C. T. Womble and M. Weck, Synthesis and Aqueous Self-Assembly of ABCD Bottlebrush Block Copolymers, *Macromolecules*,53, 9018–9025.

18 A. H. Gröschel, F. H. Schacher, H. Schmalz, O. V. Borisov, E. B. Zhulina, A. Walther and A. H. E. Müller, Precise hierarchical self-assembly of multicompartment micelles, *Nat. Commun.*, 2012, **3**, 1–10.

19 U. Tritschler, S. Pearce, J. Gwyther, G. R. Whittell and I. Manners, 50th Anniversary Perspective: Functional Nanoparticles from the Solution Self-Assembly of Block Copolymers, *Macromolecules*, 2017, **50**, 3439–3463.

20 J.-F. Lutz and A. Laschewsky, Multicompartment Micelles: Has the Long-Standing Dream Become a Reality?, *Macromol. Chem. Phys.*, 2005, **206**, 813–817.

21 J.-N. Marsat, F. Stahlhut, A. Laschewsky, H. v. Berlepsch and C. Böttcher, Multicompartment micelles from silicone-based triphilic block copolymers, *Colloid Polym. Sci.*, 2013, **291**, 2561–2567.

22 H. v Berlepsch, C. Böttcher, K. Skrabania and A. Laschewsky, Complex domain architecture of multicompartment micelles from a linear ABC triblock copolymer revealed by cryogenic electron tomography, *Chem. Commun.*, 2009, 2290–2292.

23 Z. Li, M. A. Hillmyer and T. P. Lodge, Morphologies of Multicompartment Micelles Formed by ABC Miktoarm Star Terpolymers, *Langmuir*, 2006, **22**, 9409–9417.

24 A. Anastasaki, B. Oschmann, J. Willenbacher, A. Melker, M. H. C. Van Son, N. P. Truong, M. W. Schulze, E. H. Discekici, A. J. McGrath, T. P. Davis, C. M. Bates and C. J. Hawker, One-Pot Synthesis of ABCDE Multiblock Copolymers with Hydrophobic, Hydrophilic, and Semi-Fluorinated Segments, *Angew. Chem. Int. Ed.*, 2017, **56**, 14483–14487.

25 K. Skrabania, H. v. Berlepsch, C. Böttcher and A. Laschewsky, Synthesis of Ternary, Hydrophilic−Lipophilic−Fluorophilic Block Copolymers by Consecutive RAFT Polymerizations and Their Self-Assembly into Multicompartment Micelles, *Macromolecules*, 2010, **43**, 271–281.

26 D. Heinz, E. Amado and J. Kressler, Polyphilicity—An Extension of the Concept of Amphiphilicity in Polymers, *Polymers*, 2018, **10**, 960.

27 D. Baskaran and A. H. E. Müller, in *Controlled and Living Polymerizations*, John Wiley & Sons, Ltd, 2009, pp. 1–56.

28 G. Odian, *Principles of Polymerization*, John Wiley & Sons, 2004.

29 K. Matyjaszewski and A. H. E. Müller, *Controlled and Living Polymerizations: From Mechanisms to Applications*, John Wiley & Sons, 2009.

30 C. W. Bielawski and R. H. Grubbs, Living ring-opening metathesis polymerization, *Prog. Polym. Sci.*, 2007, **32**, 1–29.

31 A. Leitgeb, J. Wappel and C. Slugovc, The ROMP toolbox upgraded, *Polymer*, 2010, **51**, 2927–2946.

32 T.-P. Lin, A. B. Chang, H.-Y. Chen, A. L. Liberman-Martin, C. M. Bates, M. J. Voegtle, C. A. Bauer and R. H. Grubbs, Control of Grafting Density and Distribution in Graft Polymers by Living Ring-Opening Metathesis Copolymerization, *J. Am. Chem. Soc.*, 2017, **139**, 3896–3903.

33 S. Kanaoka and R. H. Grubbs, Synthesis of Block Copolymers of Silicon-Containing Norbornene Derivatives via Living Ring-Opening Metathesis Polymerization Catalyzed by a Ruthenium Carbene Complex, *Macromolecules*, 1995, **28**, 4707–4713.

34 D. M. Lynn, S. Kanaoka and R. H. Grubbs, Living Ring-Opening Metathesis Polymerization in Aqueous Media Catalyzed by Well-Defined Ruthenium Carbene Complexes, *J. Am. Chem. Soc.*, 1996, **118**, 784–790.

35 D. A. Rankin and A. B. Lowe, New Well-Defined Polymeric Betaines: First Report Detailing the Synthesis and ROMP of Salt-Responsive Sulfopropylbetaine- and Carboxyethylbetaine-exo-7-oxanorbornene Monomers, *Macromolecules*, 2008, **41**, 614–622.

36 R. Walker, R. M. Conrad and R. H. Grubbs, The Living ROMP of trans-Cyclooctene, *Macromolecules*, 2009, **42**, 599–605.

37 Z. Wu and R. H. Grubbs, Synthesis of Narrow Dispersed Linear Polyethylene and Block Copolymers from Polycyclobutene, *Macromolecules*, 1994, **27**, 6700–6703.
38 J. A. van Hensbergen, R. P. Burford and A. B. Lowe, Post-functionalization of a ROMP polymer backbone via radical thiol-ene coupling chemistry, *J. Polym. Sci. A Polym. Chem.*, 2013, **51**, 487–492.
39 S. Varlas, S. B. Lawrenson, L. A. Arkinstall, R. K. O'Reilly and J. C. Foster, Self-assembled nanostructures from amphiphilic block copolymers prepared via ring-opening metathesis polymerization (ROMP), *Prog. Polym. Sci.*, 2020, **107**, 101278.
40 E. Perez, J. P. Laval, M. Bon, I. Rico and A. Lattes, Synthesis of bicyclo [2· 2· 1] hept-2-enes with mono and disubstituted long perfluorinated chains CnF2n+1 (n = 4,6,8,10) Investigation of association in solution by 19F NMR study of polymerization via a metathetic reaction, *J. Fluor. Chem.*, 1988, **39**, 173–196.
41 C. J. Faulkner, R. E. Fischer and G. K. Jennings, Surface-Initiated Polymerization of 5-(Perfluoro-n-alkyl)norbornenes from Gold Substrates, *Macromolecules*, 2010, **43**, 1203–1209.
42 K. O. Kim and T.-L. Choi, Synthesis of Dendronized Polymers via Macromonomer Approach by Living ROMP and Their Characterization: From Rod-Like Homopolymers to Block and Gradient Copolymers, *Macromolecules*, 2013, **46**, 5905–5914.
43 S. F. Alfred, K. Lienkamp, A. E. Madkour and G. N. Tew, Water-soluble ROMP polymers from amine-functionalized norbornenes, *J. Polym. Sci. A Polym. Chem.*, 2008, **46**, 6672–6676.
44 C. P. Callaway, S. M. Lee, M. Mallard, B. Clark and S. S. Jang, Effect of Block Length and Side Chain Length Ratios on Determining a Multicompartment Micelle Structure, *J. Phys. Chem. B*, 2019, **123**, 4784–4791.
45 K. Lienkamp, A. E. Madkour, A. Musante, C. F. Nelson, K. Nüsslein and G. N. Tew, Antimicrobial Polymers Prepared by ROMP with Unprecedented Selectivity: A Molecular Construction Kit Approach, *J. Am. Chem. Soc.*, 2008, **130**, 9836–9843.
46 K. Lienkamp, C. F. Kins, S. F. Alfred, A. E. Madkour and G. N. Tew, Water-soluble polymers from acid-functionalized norbornenes, *J. Polym. Sci. A Polym. Chem.*, 2009, **47**, 1266–1273.
47 T.-L. Choi and R. H. Grubbs, Controlled Living Ring-Opening-Metathesis Polymerization by a Fast-Initiating Ruthenium Catalyst, *Angew. Chem. Int. Ed.*, 2003, **42**, 1743–1746.
48 J. Xin, D. Liu and C. Zhong, Morphology and Structure Control of Multicompartment Micelles from Triblock Copolymer Blends, *J. Phys. Chem. B*, 2009, **113**, 9364–9372.
49 I. W. Wyman and G. Liu, Micellar structures of linear triblock terpolymers: Three blocks but many possibilities, *Polymer*, 2013, **54**, 1950–1978.
50 Y. H. A. Hussein and M. Youssry, Polymeric Micelles of Biodegradable Diblock Copolymers: Enhanced Encapsulation of Hydrophobic Drugs, *Materials*, 2018, **11**, 688.
51 W. K. Marek, W. Piątkowski and D. Antos, Retention Behavior of Polyethylene Glycol and Its Influence on Protein Elution on Hydrophobic Interaction Chromatography Media, *Chromatographia*, 2018, **81**, 1641–1648.
52 E. L. Hynes, J. T. Cabral, A. J. Parnell, P. Gutfreund, R. J. L. Welbourn, A. D. F. Dunbar, D. Môn and A. M. Higgins, Interfacial width and phase equilibrium in polymer-fullerene thin-films, *Commun. Phys.*, 2019, **2**, 1–13.
53 C. P. Callaway, K. Hendrickson, N. Bond, S. M. Lee, P. Sood and S. S. Jang, Molecular Modeling Approach to Determine the Flory-Huggins Interaction Parameter for Polymer Miscibility Analysis, *ChemPhysChem*, 2018, **19**, 1655–1664.
54 Malvern Instruments Limited, *Dynamic Light Scattering, Common Terms Defined*, World Wide, 2011.
55 L. Zhang and A. Eisenberg, Multiple Morphologies and Characteristics of "Crew-Cut" Micelle-like Aggregates of Polystyrene-b-poly(acrylic acid) Diblock Copolymers in Aqueous Solutions, *J. Am. Chem. Soc.*, 1996, **118**, 3168–3181.
56 K. Skrabania, A. Laschewsky, H. v. Berlepsch and C. Böttcher, Synthesis and Micellar Self-Assembly of Ternary Hydrophilic−Lipophilic−Fluorophilic Block Copolymers with a Linear PEO Chain, *Langmuir*, 2009, **25**, 7594–7601.
57 J. Zhu, S. Zhang, K. Zhang, X. Wang, J. W. Mays, K. L. Wooley and D. J. Pochan, Disk-cylinder and disk-sphere nanoparticles via a block copolymer blend solution construction, *Nat. Commun.*, 2013, **4**, 2297.
58 C. P. Callaway, N. Bond, K. Hendrickson, S. M. Lee and S. S. Jang, Structural Tunability of Multicompartment Micelles as a Function of Lipophilic–Fluorophilic Block Length Ratio, *J. Phys. Chem. B*, 2018, **122**, 12164–12172.
59 R. D. Groot and P. B. Warren, Dissipative particle dynamics: Bridging the gap between atomistic and

mesoscopic simulation, *J. Chem. Phys.*, 1997, **107**, 4423–4435.